Geophysical Journal International

Geophys. J. Int. (2010) **183,** 358–374 doi: 10.1111/j.1365-246X.2010.04731.x

Historical seismograms for unravelling a mysterious earthquake: The 1907 Sumatra Earthquake

Hiroo Kanamori,[1] Luis Rivera[2] and William H. K. Lee[3]

[1] *Seismological Laboratory, California Institute of Technology, Pasadena, CA 91125, USA. E-mail: hiroo@gps.caltech.edu*
[2] *Institut de Physique du Globe de Strasbourg; Université de Strasbourg-CNRS, Strasbourg, France*
[3] *862 Richardson Court, Palo Alto, CA 94303, USA*

Accepted 2010 July 8. Received 2010 June 29; in original form 2009 November 16

SUMMARY

History of instrumental seismology is short. Seismograms are available only for a little more than 100 years; high-quality seismograms are available only for the last 50 years and the seismological database is very limited in time. To extend the database, seismograms of old events are of vital importance. Many unusual earthquakes are known to have occurred, but their seismological characteristics are poorly known. The 1907 Sumatra earthquake is one of them (1907 January 4, $M = 7.6$). Gutenberg and Richter located this event in the outer-rise area of the Sunda arc. This earthquake is known to be anomalous because of its extensive tsunami, which is disproportionate of its magnitude. The tsunami affected the coastal areas over 950 km along the Sumatran coast. We investigated this earthquake using the historical seismograms we could collect from several seismological observatories. We examined the *P*-wave arrival times listed in the Strassburg Bulletin (1912) and other station bulletins. The scatter of the Observed−Computed traveltime residuals ranges from –30 to 30 s, too large to locate the event accurately. The uncertainty of the epicentre estimated from an S-P grid-search relocation study is at least 1° (∼110 km). We interpreted the Omori seismograms from Osaka, Mizusawa and Tokyo, and the Wiechert seismograms from Göttingen and Uppsala by comparing them with the seismograms simulated from modern broad-band seismograms of the 2002, 2008 and two 2010 Sumatra earthquakes which occurred near the 1907 earthquake. From the amplitude of Rayleigh waves recorded on the Omori seismograms we conclude that the magnitude of the 1907 earthquake at about 30 to 40 s is about 7.8 (i.e. 7.5 to 8.0). The *SH* waveforms recorded on the Göttingen and Uppsala seismograms suggest that the 1907 earthquake is a thrust earthquake at a shallow depth around 30 km. The most likely scenario is that the 1907 earthquake initiated on the subduction interface, and slowly ruptured up-dip into the shallow sediments and caused the extensive tsunami. Although their quantity and quality are limited, historical seismograms provide key quantitative information about old events that cannot be obtained otherwise. This underscores the importance of preserving historical seismograms.

Key words Seismic cycle; Tsunamis; Earthquake source observations; Subduction zone process; Dynamics and mechanics of faulting; Indian Ocean.

1 INTRODUCTION

Since the study of Newcomb & McCann (1987) seismic hazard in the Sunda arc has attracted much attention of seismologists. Recent geological studies of the history of coastal uplift and subsidence extracted from corals (Natawidjaja *et al.* 2004; Sieh *et al.* 2008) combined with detailed studies of recent great earthquakes (the $M_w = 9.2$ 2004 Sumatra-Andaman earthquake (e.g. Lay *et al.* 2005), the $M_w = 8.6$ 2005 Nias earthquake (e.g. Hsu *et al.* 2006; Konca *et al.* 2007), and the $M_w = 8.3$ 2007 Bengkula earthquake (e.g. Konca *et al.* 2008)) have clarified the rupture history along Sumatra and contributed significantly to our understanding of seismic hazard in this region.

Among all the earthquakes in the region, the 1907 earthquake (January 4, 05:19, $M = 7.6$, 2°N, 94 1/2°E, depth = 50 km, Gutenberg & Richter (1954), Fig. 1) is known to be anomalous. Despite its moderate magnitude, a report from the Royal Magnetic and Meteorological Observatory in Batavia (page 132–141, Koninklijk Magnetisch en Meteorologisch Observatorium te Batavia 1909), Visser (1922) and Newcomb & McCann (1987) noted that its tsunami affected the large areas extending nearly 950 km along the Sumatran coast. In fact, during the 2005 Nias earthquake, the

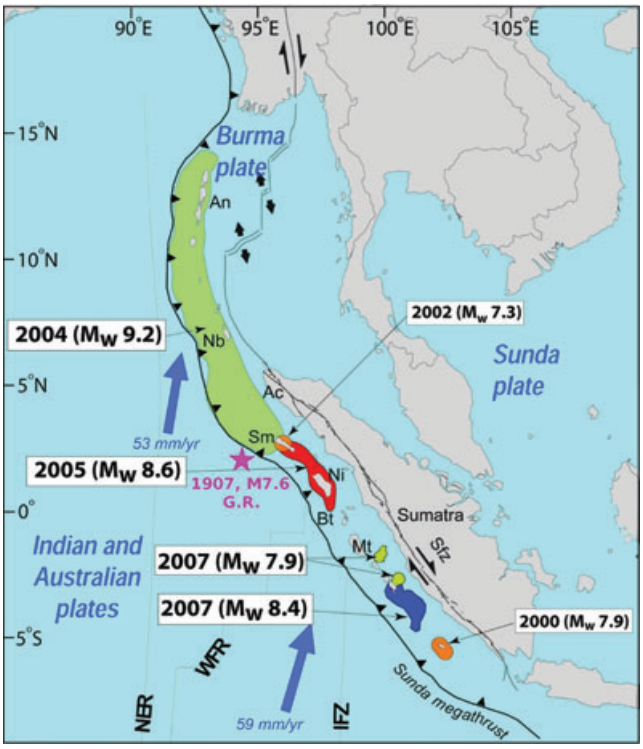

Figure 1. The location of the 1907 Sumatra earthquake and recent seismicity. (Adapted from Briggs *et al.* (2006), with inclusion of the 2007 sources from Konca *et al.* (2008). Courtesy of the Tectonic Observatory, California Institute of Technology).

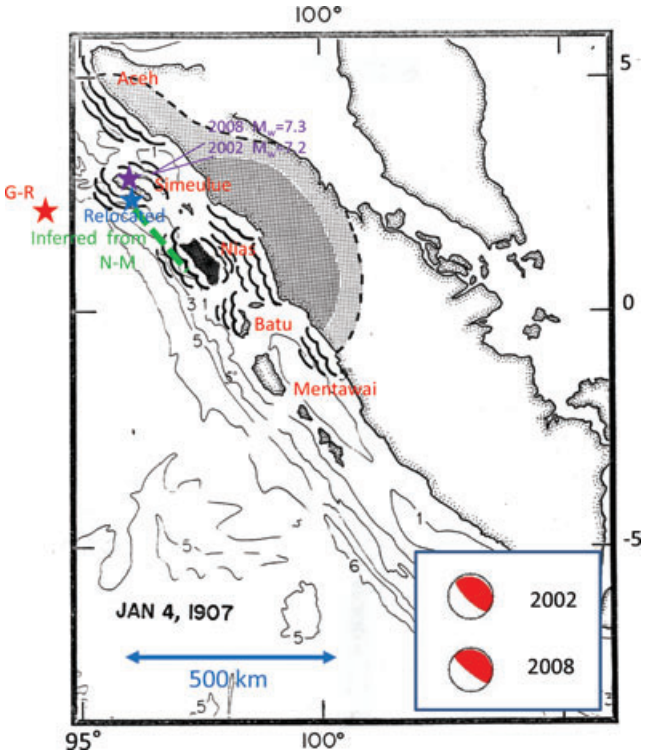

Figure 2. The areas affected by the tsunami caused by the 1907 Sumatra earthquake (modified from Newcomb & McCann (1987)). The red star shows the location given by Gutenberg & Richter (1954). The blue star indicates the relocated epicentre (see Appendix A). The purple star indicates the location of the 2002 (2.65°N, 95.99°E) and 2008 (2.69°N, 95.98°E) Sumatra earthquakes (M_w = 7.2 and 7.3, respectively) used for waveform comparison. The dashed green line indicates the inferred initial rupture zone. The inset shows the mechanisms of the 2002 and 2008 Sumatra earthquakes taken from the Global CMT solutions (http://www.globalcmt.org/CMTsearch.html).

experience with the 1907 earthquake apparently prompted the residents of the Simeulue Is. to take shelter on higher grounds immediately after they felt shaking, thereby saving many lives (McAdoo *et al.* 2006). Gutenberg & Richter (1954) located it seaward of the trench, near the outer-rise region (Fig. 1), which implies that it is not a typical subduction thrust earthquake. Unfortunately, because of the lack of sufficient instrumental data, its seismological characteristics are poorly known. Should an earthquake of this type occur somewhere today, it may pose serious tsunami and shaking hazards along the coastal areas. If the 1907 earthquake is an outer-rise earthquake, as is inferred from its location, it may cause much stronger shaking along the coastal areas than ordinary thrust earthquakes. Ammon *et al.* (2008) demonstrated that short-period ground motions with a period of 1 to 20 s from the 2007 large outer-rise earthquake in the Kuril Is. ($M_w = 8.1$) are four to seven times larger than those of the 2006 megathrust earthquake ($M_w = 8.3$) which occurred two months earlier in the same region.

In view of the importance of this earthquake, we attempted to collect as many historical seismograms as possible so that we can better understand its seismological characteristics. Unfortunately, at many seismological stations and observatories, old seismograms are rapidly being lost, partly because of deterioration of the recording paper, lack of space, or lack of maintenance personnel and infrastructure, and we could not find many records. Nevertheless, we could find a few good seismograms that proved extremely useful for unravelling some key characteristics of this unusual earthquake.

2 TSUNAMI

The anomalously large tsunami generated by this earthquake has been described by a report from the Royal Magnetic and Meteorological Observatory in Batavia (Koninklijk Magnetisch en Meteorologisch Observatorium te Batavia 1909) and Visser (1922). According to these authors, on January 4, 1907, destructive tidal waves devastated the Isle of Simaloer (Simeulue), and were observed all along the coasts of Atjeh (Aceh), Tapanoeli and the Mentawei Isles (Mentawai Is.). According to Newcomb & McCann (1987) (Fig. 2) this event caused tsunamis that devastated Simeulue Is. and extended over 950 km along the Sumatran coast. People on Nias Is. were not able to stand. Islands on the seaward side of Nias Is. and towns on the seaward side of the Batu Island were devastated by the sea wave. Monecke *et al.* (2008) note that a sand sheet of limited extent found in the tsunami deposit at Aceh might correlate with a tsunami of the 1907. Judging from these descriptions, it appears that the 1907 earthquake caused unusually widespread tsunami for an earthquake with an estimated magnitude of about 7.6. Unfortunately, we could not find any tide gauge data for this event.

3 LOCATION

Gutenberg & Richter (1954) located this event at 2°N, 94 1/2°E (depth = 50 km) (Figs 1 and 2) seaward of the Sunda trench, near the outer-rise. At a face value, this location suggests a possibility that it is a large outer-rise event. This location is very different from that (2.00°N and 96.25°E) reported by T. H. Staverman and published in

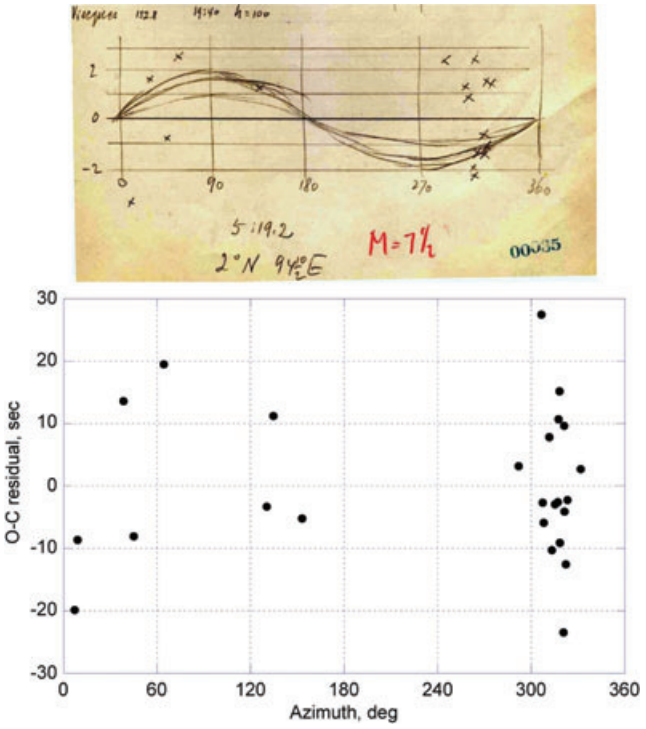

Figure 3. Top: Copy of the Gutenberg's notepad page for the 1907 earthquake, and the relocation diagram (P. 696, Richter 1958). Bottom: Observed−Computed (O–C) traveltime residuals computed from the P arrival times reported in the Strassburg Bulletin.

Szirtes (1912). Staverman probably used S-P times. We reviewed the Gutenberg's notepad (here Gutenberg's notepad refers to the original Gutenberg's notes which contain the information on the location and magnitude of the events listed in Gutenberg & Richter's (1954) Seismicity of the Earth. All available notepads were microfilmed (Goodstein *et al.* 1980), and the original copies are archived at the California Institute of Technology). Fig. 3 illustrates Gutenberg's relocation procedure. The scatter of the observed–computed traveltimes (O–C residuals) is very large. Gutenberg probably applied a weighting scheme on the basis of his experience in his attempt to locate this event, and he must have been aware of the large uncertainty in location. However, when the final location was entered in the catalog of Seismicity of the Earth, the information on the size of uncertainty was lost. Although it is difficult to accurately estimate the uncertainty in the epicentre with the large scatter of O–C residuals (Fig. 3), our S-P grid-search relocation analysis suggests that it is at least 1° (∼110 km) (see Appendix A). Although the location is very uncertain, this information is useful because it allows us to accommodate the possibility that this event could be of any type other than an outer-rise event, such as a thrust event on the plate interface.

We investigated the uncertainties in the location using S-P times from 12 well-distributed stations. The use of S-P times has advantage because it can minimize the effect of clock errors that were often very large before the 1920s (until radio timing signals became commonly available). We used the JLoc interactive, direct-search, location software (Lee & Baker 2006; Lee & Dodge 2007) using a modern velocity model, AK135 by Kennett *et al.* (1995). A focal depth is fixed at 20 km. The epicentre thus relocated is at 2.48°N and 96.11°E, and is shown in Fig. 2. Because of the large error in traveltimes, the epicentre location estimated from S-P times has an error of at least 1°. More details are given in Appendix A.

4 WAVEFORMS

We searched for old seismograms of this event by inquiring many seismic stations in the world. As is described in Appendix C (Table C1), old seismograms have been lost at many stations in the world, and despite our extensive efforts, we could find only a few Omori seismograms from Japan, and Wiechert seismograms from Europe that are useful for our analysis. Nevertheless, by examining these seismograms, we could determine a few key attributes of this earthquake. In what follows, we describe the details of the seismograms we investigated.

4.1 Osaka (34.70°N, 135.52°E)

Fig. 4 shows the Omori seismogram recorded at Osaka, Japan. Although the original seismogram was discarded, a hand-copied seismogram was published in the Report of Osaka Observatory (Report on Omori Horizontal Pendulum Seismograph Observations in Osaka for the two years 1906–1907 published by Osaka Observatory 1908). According to the Report, the Omori seismograph at Osaka had a free period, T_0, of 27s, and the static magnification, V, of 20. Omori seismographs did not have any specific damping device, and the actual damping was probably due to air friction, and solid frictions at the pivot and the recording stylus. Occasionally, a calibration signal is given either in the beginning or at the end of the record from which the damping ratio ε can be estimated (Richter 1958, page 216). Unfortunately, no calibration signal is recorded on this seismogram. Four distinct wave trains can be identified on the seismogram. As we will show later, they can be identified as P, S, 'Love', and Rayleigh waves. 'Love' means that it is a combination of multiple S phases and Love waves. In those days, the polarity of the seismogram was seldom written on the record, but this record has polarity clearly marked: upward motion on the record means westward ground motion.

To interpret this seismogram, we compared it with a simulated Omori seismogram computed from a broad-band seismogram of the 2002 Sumatra earthquake (2002 November 2, 2.65°N; 95.99°E, 23 km, $M_w = 7.2$) recorded at ABU (Abuyama, Japan, 34.864°N, 135.571°E, 138 m). This earthquake is a thrust earthquake that occurred in the same area as the 1907 earthquake (Fig. 2). The distance between Osaka and ABU is 17 km.

The simulation was made by removing the instrument response from the E-W component of the broad-band record, and convolving it with the response of the Omori seismograph. As mentioned above, the effective damping of the Omori seismograph is not known. Thus, we vary the damping constant h from 0.05 to 0.4, compare the computed seismograms with the observed (Fig. 5), and chose h that yields a seismogram most similar to the observed. The damping ratio ε is related to the damping constant h by $\varepsilon = \exp(\frac{\pi h}{\sqrt{1-h^2}})$. We found that $h = 0.2$ is most appropriate, but inevitably some uncertainty is involved in this choice. As h decreases, the amplitude of simulated seismogram increases. If $h = 0.1$ and 0.3, then the amplitude of the simulated seismogram becomes 1.31 and 0.83 times, respectively, of that for $h = 0.2$. This range will be considered in estimating the magnitudes. The simulated Omori seismogram for the EW component record at Osaka is shown on Fig. 4. The overall waveform of the observed record is similar to that of the simulated record in terms of the relative amplitude of P, S, Love, and Rayleigh waves, which suggests that the fault geometry of the two events is similar.

Fig. 6 shows the radiation patterns of P, SV, SH, and surface waves (both Love and Rayleigh waves) computed for the mechanism

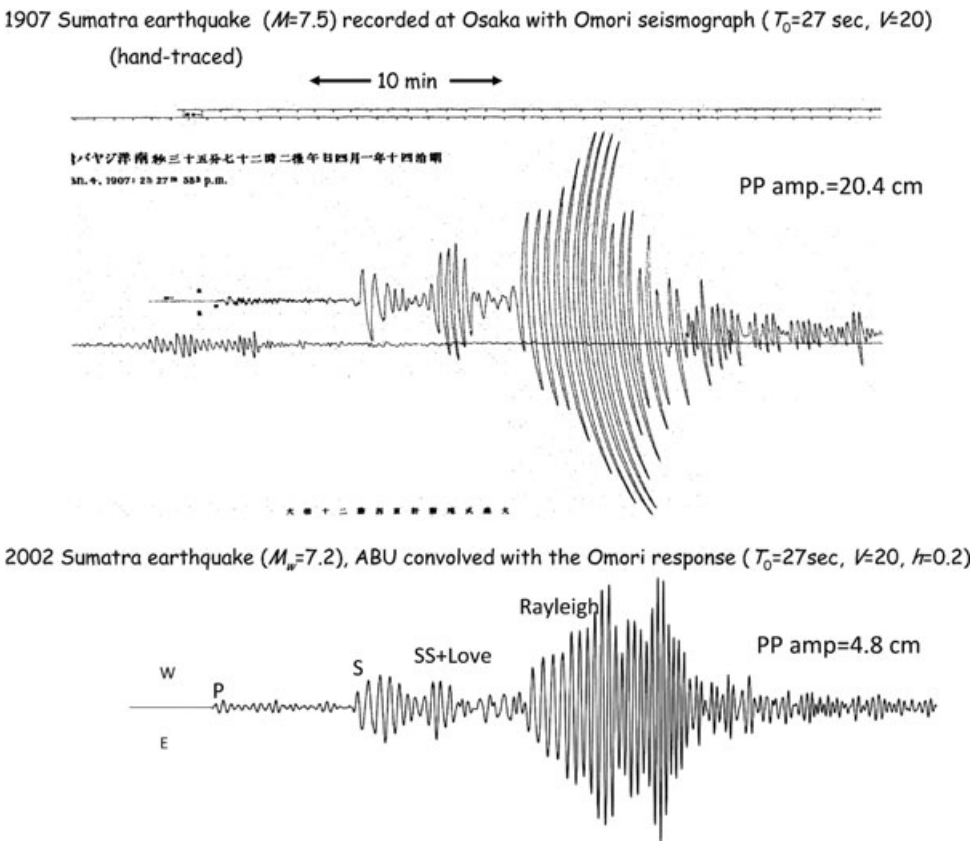

Figure 4. Comparison of the Omori seismogram (EW component) of the 1907 Sumatra earthquake recorded at Osaka, Japan, with a simulated Omori seismogram computed from the seismogram of the 2002 Sumatra earthquake ($M_w = 7.2$) recorded at ABU (Abuyama), Japan. Here a damping constant, h, of 0.2 is assumed.

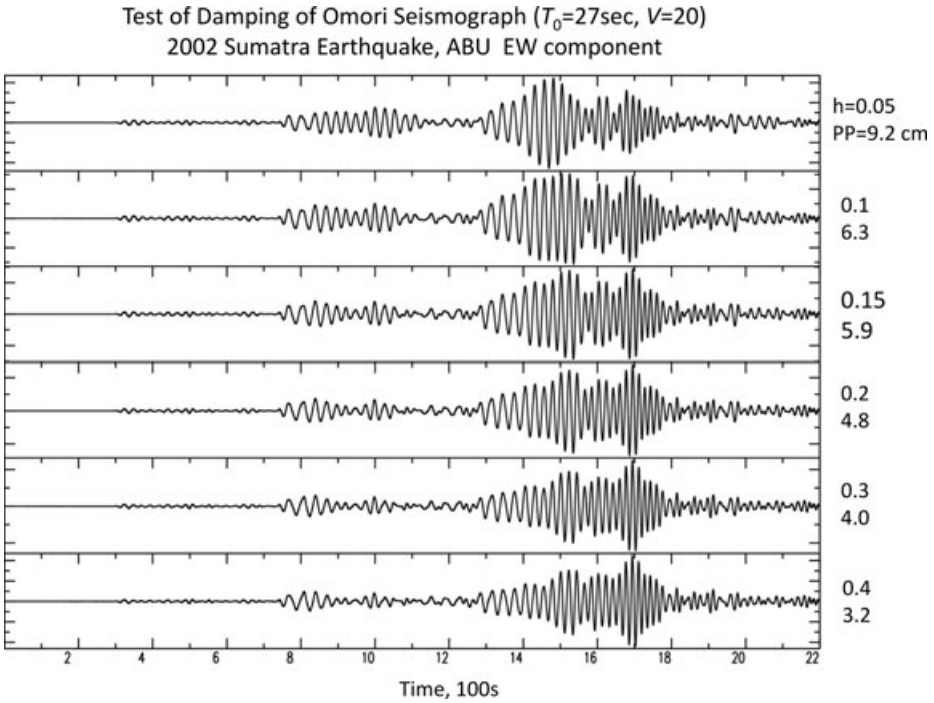

Figure 5. The effect of damping constant, h, on the amplitude and waveform of simulated Omori seismograms computed from the broad-band record of the 2002 Sumatra earthquake recorded at ABU (Abuyama, Japan). The damping constant, h, and the peak-to-peak amplitude of the wave at the free period are given on the right. For $h < 0.1$, the S group and Love wave become too continuous compared with the observed. To distinguish the waveforms for $h = 0.2$, 0.3, and 0.4 is difficult, but h much larger than 0.3 is unlikely for an instrument without any specific damping device. The peak-to-peak amplitudes of the wave at the free period are 6.3, 4.8, and 4.0 for $h = 0.1$, 0.2, and 0.3, respectively.

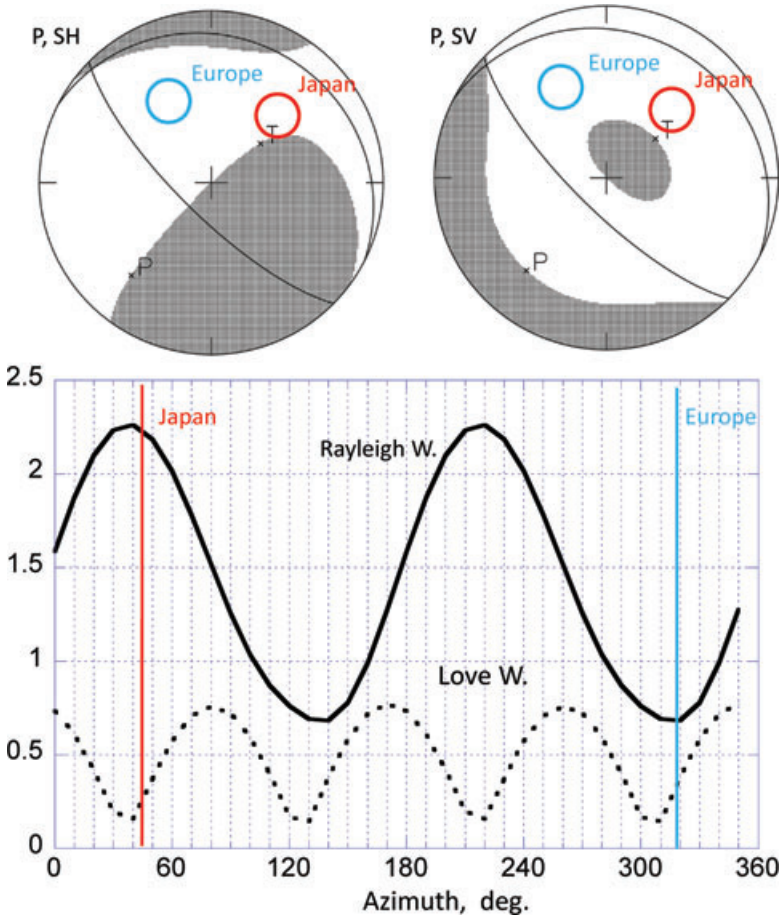

Figure 6. Top: The radiation patterns of P, SH, and SV phases for the 2002 Sumatra earthquake. The orthogonal nodal planes are shown for *P* wave, and the positive and negative *SH* and *SV* waves are shown by blank and filled areas. The locations of the Japanese and European stations used in this paper are sketched on the stereographic diagrams. Bottom: Schematic radiation patterns of Rayleigh and Love waves as a function of azimuth for the 2002 Sumatra earthquake. The amplitude is in an arbitrary unit; only the pattern is relevant here.

of the 2002 Sumatra earthquake. Japan is located in the direction close to the nodes of SH and Love wave radiation patterns, but is close to the peak of Rayleigh-wave radiation pattern. Thus, the Rayleigh-wave amplitude is robust with respect to small changes in the mechanism.

The observed Rayleigh-wave amplitude is about 4 times larger than the simulated, suggesting a surface-wave magnitude difference of 0.6. However, because of the uncertainty in h, the magnitude estimate is correspondingly uncertain. We will estimate the magnitude later using all the seismograms we investigated.

The *P*-wave first motion on the observed record appears to be eastward, which means an 'up' first-motion. Since the *P*-wave first motion in Japan from low-angle megathrust earthquakes in Sumatra is 'up' (Fig. 6), and that of outer-rise normal-fault earthquakes is most likely 'down', this observation suggests that this event is probably a thrust event rather than a normal-fault event.

4.2 Mizusawa, Japan (39.13°N, 141.13°E)

Fig. 7 shows the Omori seismogram of the 1907 Sumatra earthquake recorded at Mizusawa, Japan. The free period, T_0, and the magnification, V, are 30 s and 20, respectively. We made a similar comparison of this record with a simulated seismogram computed from the seismogram of the 2002 Sumatra earthquake recorded at the station KSN (Kesen-numa, Japan, 38.976°N, 141.530°E, 260 m). The distance between Mizusawa and Kesen-numa is 39 km. In general, major features of the observed and the simulated records are similar, confirming the conclusion obtained from the Osaka record. The ratio of the observed to simulated peak-to-peak amplitudes of the Rayleigh wave is about 4.3, which translates to a magnitude difference of 0.6.

Fig. 8 shows a similar comparison for the NS component. The gain of the NS component is much lower, 9, than the EW component for unknown reason. A strange observation is that the Love wave is not obvious on this component. Since the backazimuth at Mizusawa is 240°, Love wave should be stronger on the NS component regardless of the mechanism. This observation remains unexplained, but *S* and Love waves are nodal at Mizusawa; we use only Rayleigh waves for the amplitude comparison.

4.3 Tokyo, Japan, (35.71°N, 139.77°E)

At Hongo in Tokyo, several Omori seismographs were in use (Omori 1907). Fig. 9 is the one in Tokyo at the Seismological Institute of Tokyo Imperial University where Professor Omori was working. This is probably the same record as that Professor Omori investigated himself. The period, T_0, and the magnification, V, are 41.5 s and 30, respectively.

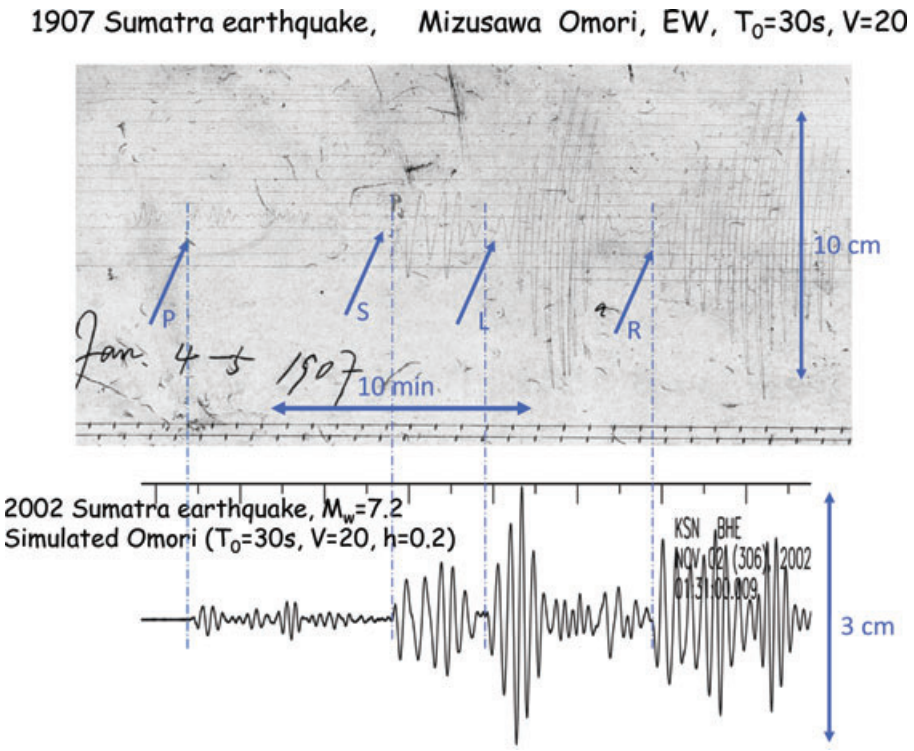

Figure 7. Comparison of the Omori seismogram (EW component) of the 1907 Sumatra earthquake recorded at Mizusawa, Japan, with a simulated Omori seismogram computed from the seismogram of the 2002 Sumatra earthquake ($M_w = 7.2$) recorded at KSN (Kesen-numa, Japan).

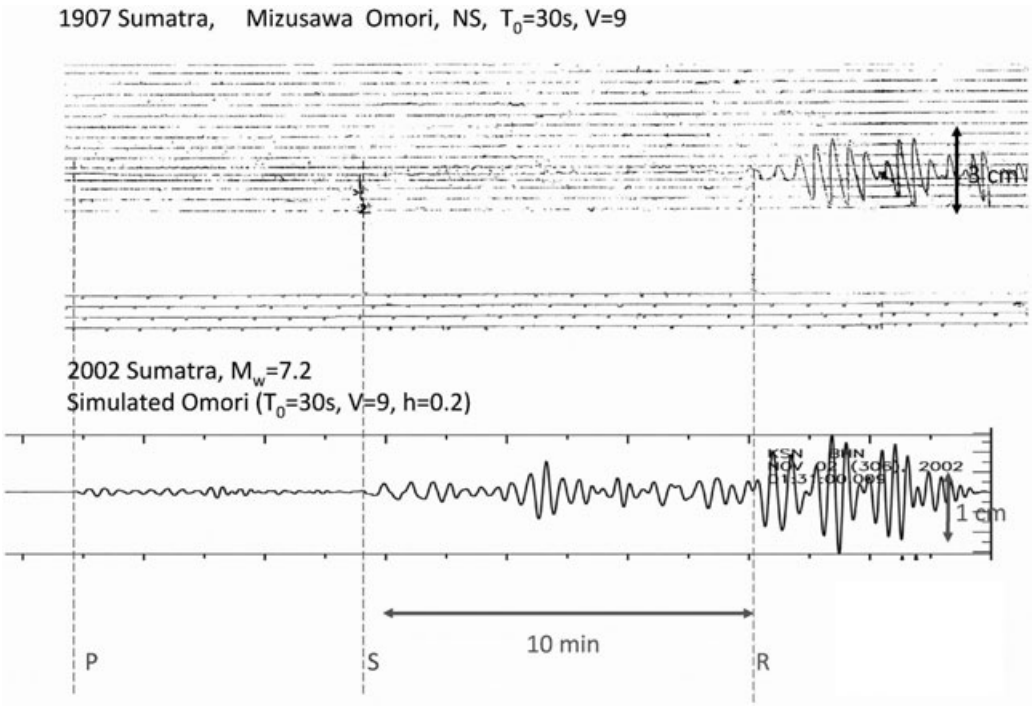

Figure 8. Comparison of the Omori seismogram (NS component) of the 1907 Sumatra earthquake recorded at Mizusawa, Japan, with a simulated Omori seismogram computed from the seismogram of the 2002 Sumatra earthquake ($M_w = 7.2$) recorded at KSN (Kesen-numa, Japan).

We computed a simulated record from a broad-band seismogram at TSK (Tsukuba, 36.214°N, 140.090°E, 174 m) of the 2008 Sumatra earthquake (2008 February 20, 2.69°N; 95.98°E, 15 km, $M_w = 7.3$) which is located close to the 2002 Sumatra earthquake (Fig. 2). The 2002 Sumatra earthquake was not recorded at TSK. The distance between Tokyo and Tsukuba is 63 km. The correspondence between the observed and simulated record is excellent. Since the Rayleigh wave went off scale, we cannot measure the amplitude

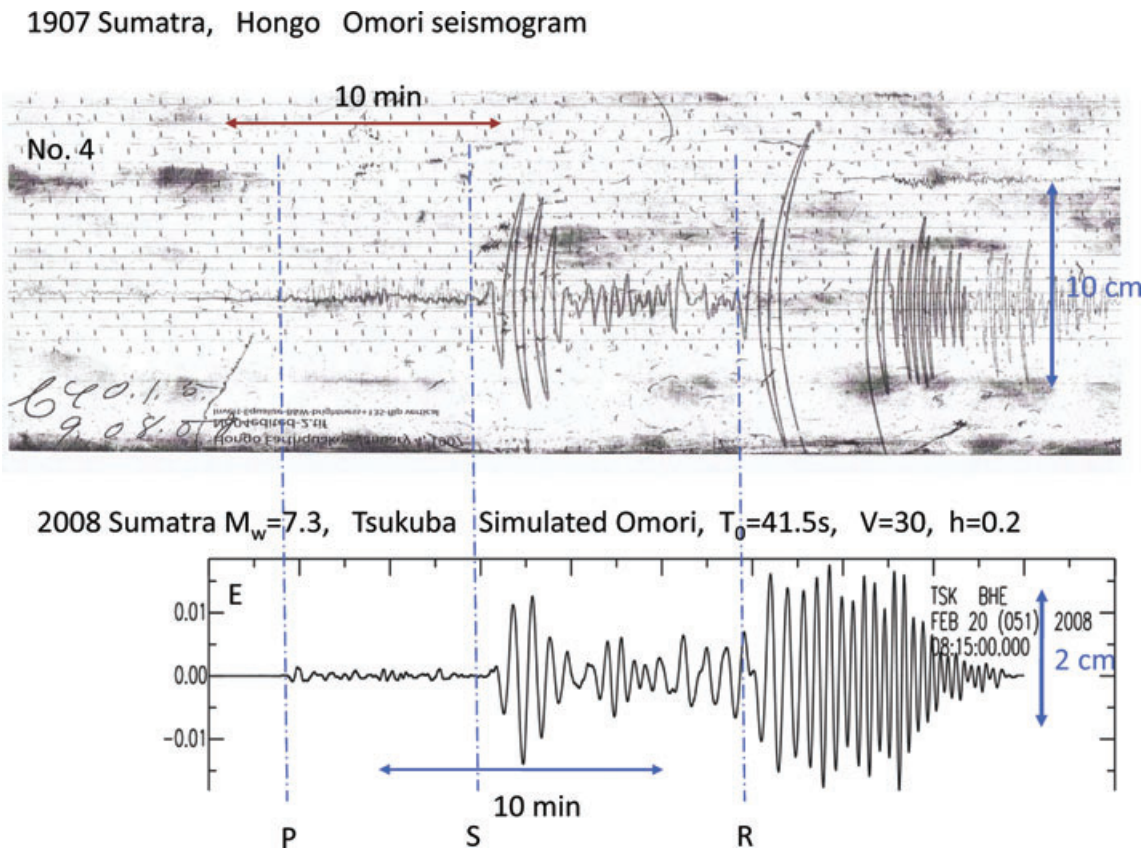

Figure 9. Comparison of the Omori seismogram (EW component) of the 1907 Sumatra earthquake recorded at Hongo, Tokyo Japan, with a simulated Omori seismogram computed from the seismogram of the 2008 Sumatra earthquake ($M_w = 7.3$) recorded at TSK (Tsukuba, Japan).

ratio, but the observed to the simulated ratio is at least 4.9, suggesting that the surface-wave magnitude of the 1907 earthquake is at least 0.7 units larger than that of the 2008 earthquake.

Fig. 10 shows an NS component Omori seismogram recorded at Hongo. This is one of few NS component seismograms; most of the old Omori seismograms at Hongo now archived are EW component. On this record, a calibration signal is recorded at the bottom of the record from which we could estimate the damping ratio ε (or damping constant h). Comparing the appearance of this seismogram with the one on Fig. 9, we can immediately see the difference in damping. The seismogram on Fig. 10 is close to a harmonic oscillation with the free period (40.0 s). The damping constant h estimated from the calibration signal is approximately 0.05. Although the waveforms of the observed and simulated records are very similar, the amplitude measurement is not reliable because of the extremely small damping. A small error in h results in a large difference in the amplitude of the simulated record. The ratio of the observed to the simulated Rayleigh-wave amplitudes is only 1.2 with a corresponding magnitude difference of only 0.1.

4.4 Göttingen, Germany (51.550°N, 9.967°E), Uppsala, Sweden (59.850°N, 17.635°E), Potsdam, Germany (52.383°N, 13.067°E), and Hamburg, Germany (53.567°N, 9.983°E)

Fig. 11 shows the two component Wiechert seismograms made available to us by courtesy of the Göttingen Observatory. The polarity of the Göttingen seismograms is clearly marked as N and E for downward motion on the record. The seismograph constants are: NS $T_0 = 12.8$s, $\varepsilon = 4.2$, $V = 156$; EW $T_0 = 13.3$, $\varepsilon = 5.6$, $V = 156$. The most notable is the sharp S wave recorded on the NS component. Also shown on this figure are the two-component simulated Wiechert seismograms computed from the seismograms of the 2002 Sumatra earthquake recorded at the station BFO, Germany (48.332°N, 8.331°E). Since the backazimuth at Göttingen from the 2002 Sumatra earthquake is 98.5°, the NS component is essentially the transverse component. The overall similarity between the 1907 and 2002 seismograms concerning the energy partition between NS (SH component) and EW (SV component) and the large sharp *SH* wave on the NS component is evident, which suggests that the 1907 and the 2002 events have a similar mechanism.

The copies of the Wiechert seismograms of the Uppsala Observatory are faint, but the S wave on the NS component is traceable (Fig. 12). Unfortunately, the polarity is not marked on the Uppsala seismograms. Different Wiechert seismographs can have different polarity settings and all the possible combinations (upward = East, upward = West, upward = North, upward = South) are indeed found in the old Wiechert seismographs operating early in the 20th century around the world (Charlier & Van Gills 1953; M. Cara, personal communication, 2007). According to Bungum *et al.* (2009), their test using the first-motion direction of the events with 'known polarity' and a direct test on the Uppsala seismograph indicated that upward motion on the NS and EW component records corresponds to southward and westward ground motion, respectively. We confirmed their result by checking the polarity of the P-wave first motion of the 1933 Sanriku, Japan, earthquake ($M_w = 8.4$). The studies of Matuzawa (1942) and Kanamori (1971) indicate that the P-wave first motion at

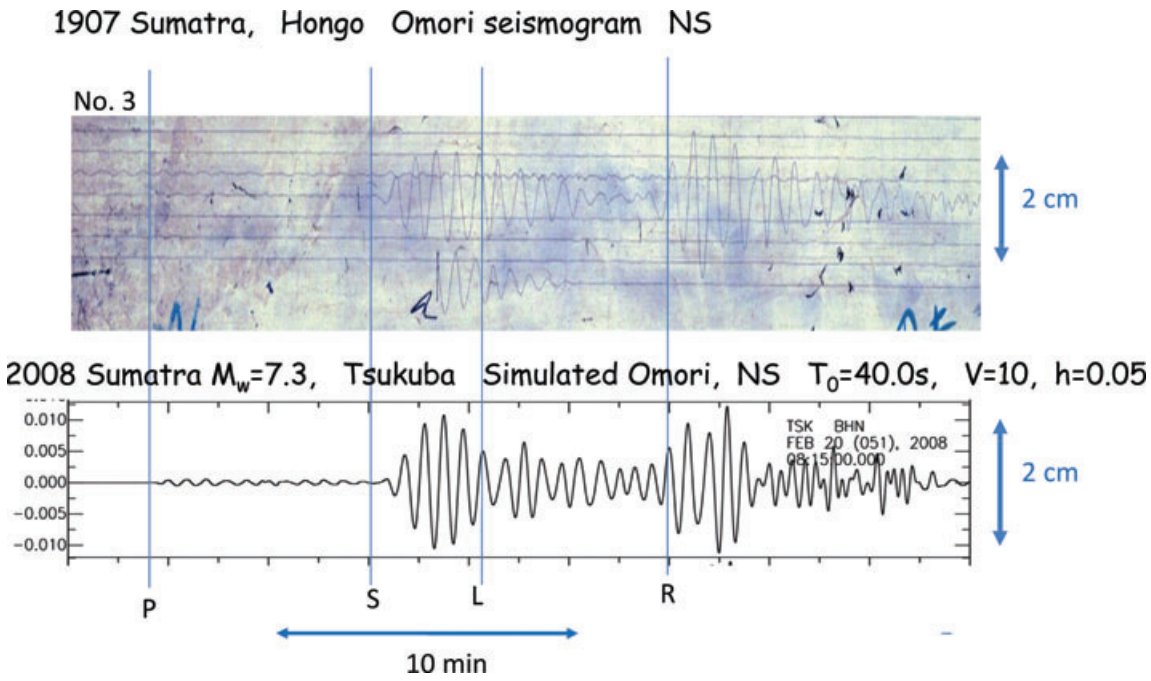

Figure 10. Comparison of the Omori seismogram (NS component) of the 1907 Sumatra earthquake recorded at Hongo, Japan, with a simulated Omori seismogram computed from the seismogram of the 2008 Sumatra earthquake ($M_w = 7.3$) recorded at TSK (Tsukuba, Japan). Here, a damping constant, $h = 0.05$ is estimated from the calibration signal on the record.

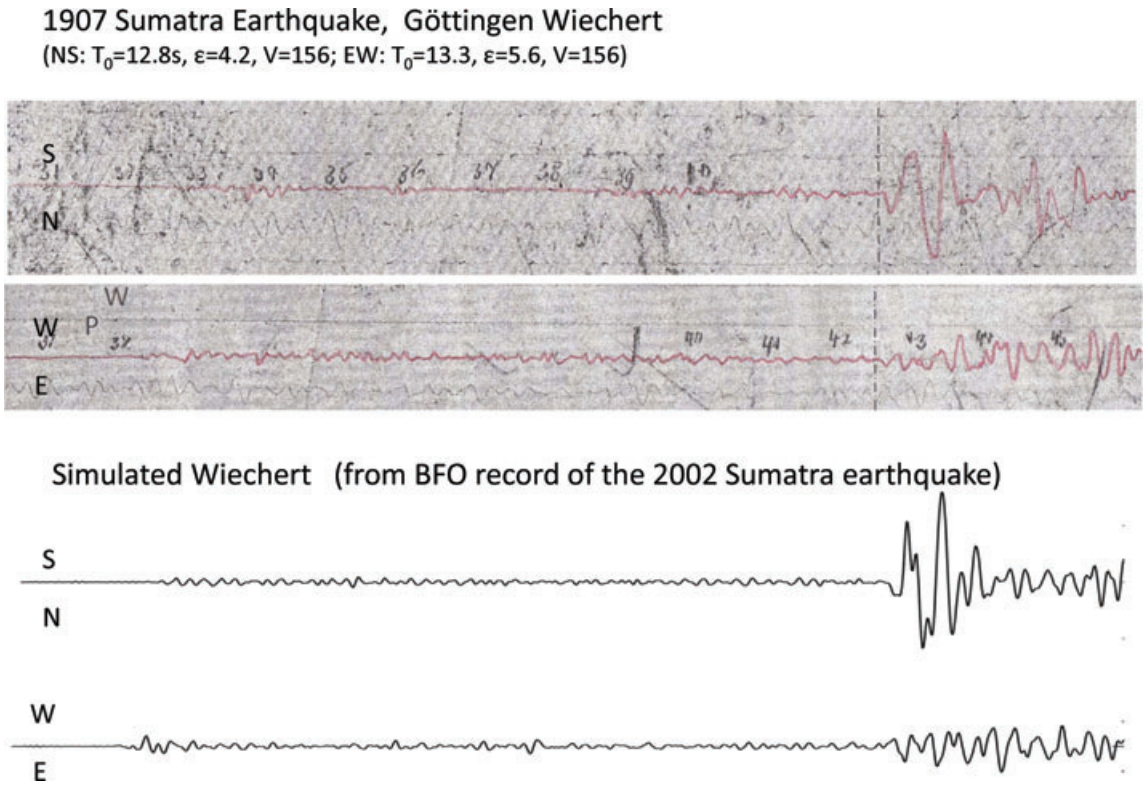

Figure 11. Comparison of the NS and EW components of the 1907 Sumatra earthquake recorded at Göttingen, Germany, with simulated Wiechert seismograms computed from the seismogram of the 2002 Sumatra earthquake recorded at BFO (Black Forest Observatory, Germany). Note the overall similarity of the energy partition between NS (SH) and EW (SV) components, and the large S wave on the NS component.

Uppsala for this earthquake must be 'north', and the recorded motion on the NS component is down. Fig. 12 compares the NS component of the Göttingen seismogram and the Uppsala seismogram ($T_0 = 10$s, $\varepsilon = 5$ (i.e. $h = 0.46$), and $V = 182$).

The seismogram we obtained from the Potsdam station is not marked at all regarding the type of instrument, component, and polarity. However, judging from the waveform, we assumed that it is the NS component (S is up on the record) Wiechert seismogram,

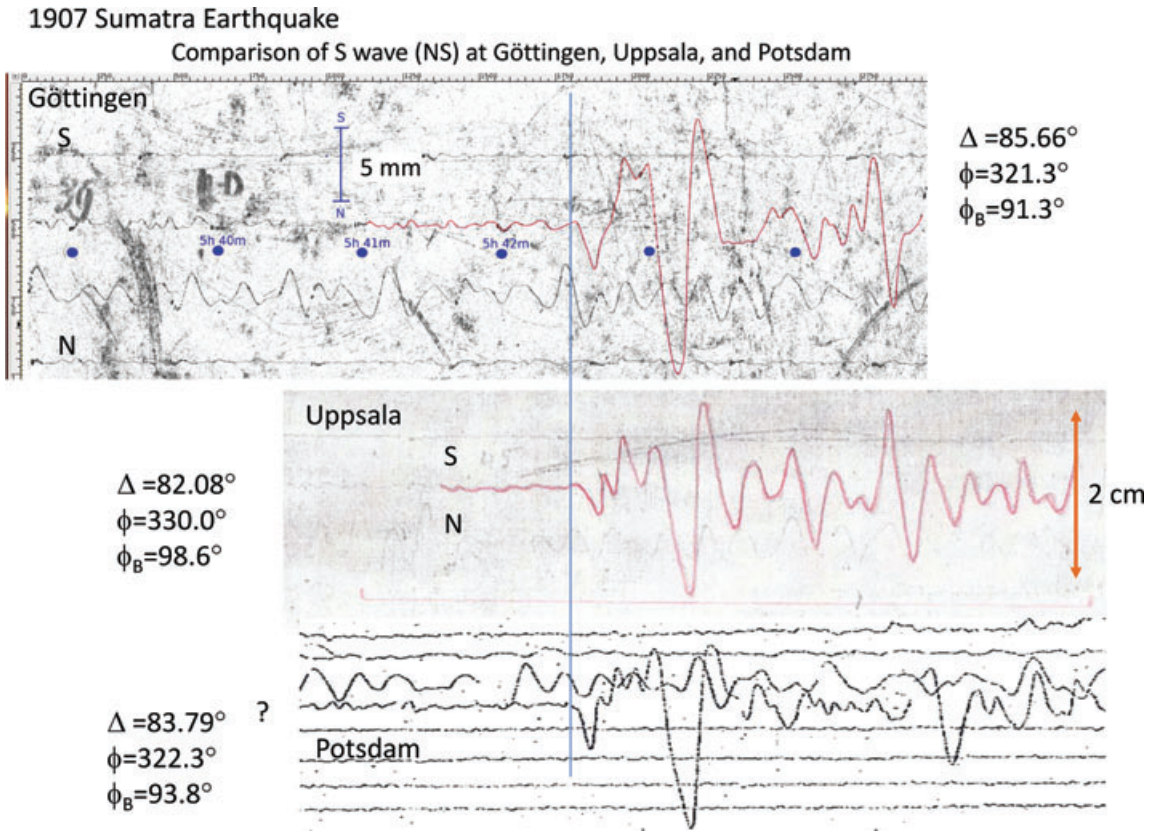

Figure 12. Comparison of the S wave on the NS component seismograms at Göttingen and Uppsala. Note the similarity of the waveform, and the northward first motion. The Potsdam seismogram is shown just for comparison.

and include it on Fig. 12 in comparison with the records from Göttingen and Uppsala. This record is not used for analysis but is shown only for comparison purposes. The first few cycles of *S* wave are similar between Göttingen and Uppsala. The Potsdam record is also similar suggesting that our assumption is probably correct.

Fig. 13 compares the NS component of *S* waveform recorded on the Göttingen seismogram with the simulated Wiechert seismogram computed from the record of the 2002 Sumatra earthquake recorded at BFO. As shown in Fig. 12 the first motion of *S* wave is northward at both Göttingen and Uppsala, and is the same as that of the 2002 Sumatra earthquake; this suggests that the 1907 earthquake is a thrust event similar to the 2002 event. This supports the somewhat weaker conclusion we made earlier from the first motion recorded at Osaka.

The waveform similarity deteriorates for the second pulse. This could be due to the difference in depth, source pulse shape, etc. To illustrate the situation, we show on the lower-left corner of Fig. 13 the moment-rate function of the 2002 event obtained by inversion of 64 P waveforms. The half duration is about 15s. The difference in the frequency content between the 1907 and 2002 events suggests that the moment-rate function for the 1907 event can be slightly broader. A synthetic waveform computed for a point source at a depth of 30 km having a triangular moment-rate function with a half duration of 20 s can match the polarity of the second pulse as shown in Fig. 13. Thus, the waveform mismatch can be partially due to a small difference in the source moment rate function between the 1907 and 2002 events.

Fig. 14 shows the *S* waveforms simulated from the seismograms of four recent Sumatra earthquakes recorded at BFO (2002 November 2, $M_w = 7.2$, $d = 23$ km, 2008 February 2, $M_w = 7.3$, $d = 14.9$ km, 2010 April 6, 2.05°N, 96.71°E, $M_w = 7.8$, d = 19.7 km, and 2010 May 9, 3.38°N, 95.79°E, $M_w = 7.2$, $d = 38$ km). These events are located close to each other with the depths from 14 to 38 km (GCMT: http://www.globalcmt.org), probably on the subduction-zone plate interface (Sladen *et al.* 2009; Tilmann *et al.* 2010). Although the displacement records of these events are relatively simple and similar to each other, the simulated Wiechert records are complex and cannot be related to the depth in a simple way. Thus, it is difficult to estimate the depth of the 1907 event accurately from the waveform, but the waveform complexity of the 1907 event suggests that this event is comparable in depth to these 4 Sumatra earthquakes, and is located on the plate boundary interface. We use 30 km as a nominal depth of the 1907 earthquake, but the implied uncertainty is from 14 to 38 km, the range of the four Sumatra earthquakes.

The amplitude ratio of the SH wave of the 1907 to the 2002 event is approximately 2.0 and 1.8 at Göttingen and Uppsala, respectively (the simulated Wiechert seismogram for Uppsala is not shown, but is similar to that for Göttingen).

Another interesting observation is that while the waveforms during the first 100 s are similar, the record of the 1907 event exhibits significant amounts of energy for another 100 s (Figs 11 and 12), during which no significant energy is seen on the record of the 2002 event. This suggests that the 1907 earthquake had an extended rupture following the initial rupture.

The Hamburg Wiechert seismograms show *S* waves and surface waves, but the traces are tangled up and hard to trace and timing marks are difficult to read. We used these records only for magnitude determination.

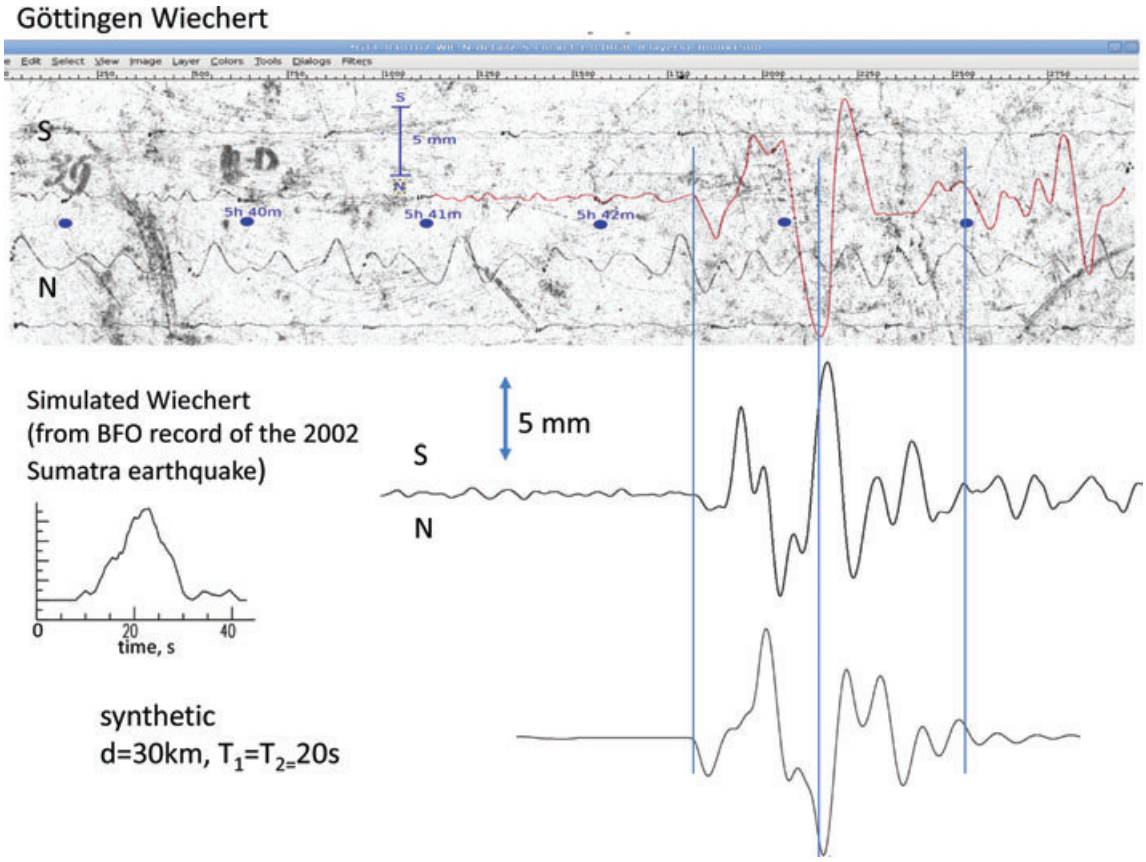

Figure 13. Comparison of the S waveform recorded at Göttingen (top) and a simulated Wiechert seismogram computed from the seismogram of the 2002 Sumatra earthquake recorded at BFO. Note that the first motion is northward for both the 1907 and 2002 events, suggesting that the 1907 earthquake had a thrust mechanism. The waveform agreement deteriorates in the second pulse. This could be due to the difference in depth, source pulse shape, etc. The moment rate function for the 2002 earthquake shown on the lower-left corner has a half duration of about 15 s. The difference in the frequency content between the 1907 and 2002 events suggests that the moment-rate function for the 1907 event can be slightly broader. The bottom trace is a synthetic waveform computed for a point source with a half duration of 20 s at a depth of 30 km.

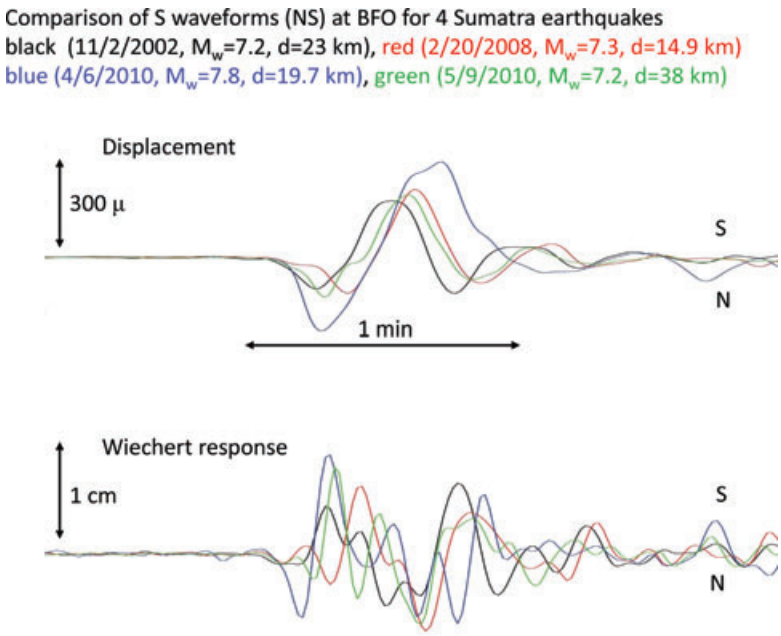

Figure 14. Comparison of S waveforms (NS component) at BFO for four Sumatra earthquakes at depths from 14 to 38 km. Top: Displacement records. Bottom: Simulated Wiechert seismograms computed with the instrument constants of the NS component of the Göttingen Wiechert seismograph.

Table 1. (a) Magnitude estimations from Omori seismograms; (b) Magnitude estimations from Wiechert Seismograms; (c) Estimation of m_B from Wiechert seismograms.

(a) Station	Component	Amplitude ratio	ΔM_S	M_S
Osaka	EW	3.2 to 5.1	0.5 to 0.71	7.65 to 7.86
Mizusawa	EW	4.3 to 6.7	0.63 to 0.83	7.78 to 7.98
Mizusawa	NS	1.4 to 2.1	0.15 to 0.32	7.30 to 7.47
Hongo	EW	>5.4 to 8.5	>0.73 to 0.93	>7.96 to 8.16
Hongo	NS	1.24	0.09	7.14
(b) Station	**Component**	**Amplitude (μm)**	**Period (s)**	**M_S**
Uppsala	NS	350	20	7.56
	EW	171	20	
Hamburg	NS	700	20	7.6
	EW	400		
(c) Station	**Component**	**Amplitude (μm)**	**Period (s)**	**m_B**
Uppsala	NS	90.7	17	7.3
Göttingen	NS	191	26	7.7

5 SUMMARY OF MAGNITUDE ESTIMATES

Table 1 summarizes the results of amplitude measurements. We estimated the magnitude difference from the amplitude ratios of the observed to simulated records, and estimated the surface-wave magnitude, M_S, using the reference values for the 2002 ($M_S = 7.15$) and 2008 ($M_S = 7.25$) Sumatra earthquakes (Appendix B). Since the damping of the NS component of the Hongo record is very small, we consider the M_S estimate from this record unreliable. Disregarding this estimate and considering the lower bound estimated from the EW component at Hongo, we prefer a range $7.5 < M_S < 8.0$ (Table 1a).

The amplitude measurements from the Wiechert seismograms at Uppsala and Hamburg are summarized in Table 1b. The Uppsala seismograms came with a detailed calibration sheet, and the amplitude measurements are considered reliable. The Hamburg seismograms did not come with calibration, and we assume a gain, 20, at a period of 20 s, which is the value for this type of Wiechert seismograph. For these determinations, the traditional Gutenberg's (1945) formula, $M_S = \log(A_H) + 1.656 \log \Delta + 1.818$ is used. The M_S values from these records agree well with that listed in Gutenberg & Richter (1954). However, as shown in Figs 6 and A1, the European stations are in the nodal azimuth of Rayleigh waves. If we correct for this effect from Figure A1, $M_S = 7.8$ is probably more appropriate.

From the amplitude of the SH wave recorded at Uppsala and Göttingen (Table 1c), we obtain $m_B = 7.3$, and 7.7, respectively. The m_B value at Göttingen was obtained at a longer period than at Uppsala. These values are comparable to what are expected of an ordinary $M_S = 7.8$ earthquake (Gutenberg 1956).

In summary, combining all these results, we estimate $M_S = 7.8$, with an uncertainty range of $+-0.25$. From the m_B and M_S relation, the 1907 event does not seem to be particularly anomalous regarding the source radiation spectrum up to a period of 30 s. However, there is some indication that the Omori EW seismogram at Hongo that has a longer free period (40 s) than the others gave a larger M_S (>7.96). The body-wave magnitudes at Uppsala and Göttingen display a similar trend. These observations together could be taken as evidence for the 1907 earthquake having an enhanced excitation at longer periods.

6 THE RUPTURE PROCESS

Although the quality of old data is limited, we can synthesize the analyses presented above and the description of macroseismic data by Visser (1922) and Newcomb & McCann (1987) as follows.

The location determined from teleseismic traveltimes is uncertain, and the uncertainty of the epicentre estimated from an S-P grid-search relocation study (Appendix A) is at least 1° (~110 km). The comparison of the Wiechert seismogram recorded at Göttingen and Uppsala and that simulated from the record of the 2002 Sumatra earthquake suggests that the initial rupture of the 1907 event is a thrust event at a depth of approximately 30 km, and it was followed by an extended rupture for at least 100s. From this observation alone we cannot determine where the extended rupture was, but referring to Newcomb and McCann (1987) it is most likely seaward of the Nias and Simeulue Islands. According to Newcomb & McCann (1987), the islands on the seaward side of Nias and towns on the seaward side of Batu Island were devastated by the sea wave. The green dashed line in Fig. 2 schematically shows the approximate initial rupture zone thus inferred. From our seismic data with the frequency band up to 40 s, we cannot determine the total size (i.e. M_w) of this event, but the magnitude determined at a period of up to 40 s is probably between 7.5 and 8. The extent of the tsunami damage (950 km) suggests that the M_w can be significantly larger than this, but without tide gauge data we cannot estimate it.

7 DISCUSSION

The 1907 Sumatra earthquake has all the attributes of tsunami earthquakes (Kanamori 1972) and is similar to the 1896 Sanriku, Japan, earthquake and the 1946 Unimak Is., the Aleutians, earthquake. According to Visser (1922) and Newcomb & McCann (1987), the 1907 earthquake caused strong shaking on the Nias and Simeulue Islands, but the intensities on Sumatra were only moderate. Although no strong shaking was reported for most other tsunami

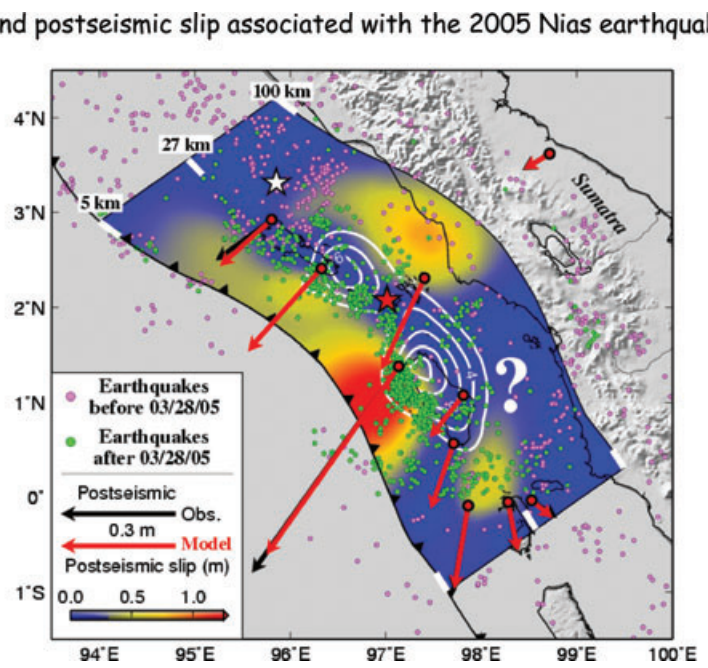

Figure 15. Coseismic and postseismic slip models for the 2005 (March 28) Nias earthquake ($M_w = 8.6$). (after Hsu *et al.* 2006; Courtesy of Dr. Yaru Hsu)

earthquakes including the 1896 Sanriku, the 1946 Unimak Is., the 1992 Nicaragua earthquake, the 1994 Java earthquake, and the 2006 Java earthquake, these subduction zones do not have islands in the forearc region over the shallow portion of the megathrust. Thus, despite the difference in the report of strong shaking, the 1907 earthquake may be similar to other tsunami earthquakes.

It is interesting to compare the 1907 event with the March 28, 2005, Nias earthquake. Although the Nias earthquake is a great earthquake with $M_w = 8.6$, no anomalously large tsunami was generated. Hsu *et al.* (2006) made a detailed study of this earthquake using seismic and static (GPS, INSAR, Coral) data and obtained the result shown in Fig. 15. The coseismic slip extended over nearly 300 km right underneath the Nias-Smeulue island chain, and significant afterslip occurred on the plate boundary between the Nias Island and the trench. However, no large coseismic slip occurred in the up-dip part of the plate boundary. In contrast, the large tsunami associated with the 1907 earthquake is most likely caused by a slip in the up-dip part of the subduction boundary. It is possible that at the time of the Nias earthquake in 2005, not enough strain had accumulated there since 1907 to cause extensive tsunami. Briggs *et al.* (2006) also note this possibility.

Earthquakes like the 1907 earthquake are less likely to leave distinct uplift and subsidence records in corals because the primary deformation was in a relatively narrow zone along the trench, being far from the coast. However, in assessing the seismic and tsunami hazard, it would be important to include the events like the 1907 earthquake that pose extremely serious tsunami hazard to the populations in the coastal area.

The 1907 earthquake is somewhat similar to the 1605 Keicho earthquake (called 'Keicho' because it occurred in the Keicho era in the Japanese calendar) along the Nankai trough. Along the Nankai trough, a series of great earthquakes have repeatedly occurred with an average interval of 120 years (Imamura 1928; Ando 1975; Ishibashi 1981). However, the 1605 event is known to be anomalous, in that despite the limited extent of shaking, it generated extensive tsunamis along the Japanese Islands. If the 1907 event released the strain which had accumulated on a shallow boundary over a long period of time, much longer than the average repeat time of regular large megathrust events like the 2005 Nias and 2007 Bengkulu earthquakes, the rupture sequence of the 1907 type earthquakes can be very different from that of the 2005 Nias type earthquakes even if they occur in the same region. Without knowledge on the detailed rupture process of old earthquakes, it would be difficult to separate these two groups of earthquakes and both types of events tend to be treated together to estimate the average repeat time. The 1605 earthquake may have to be considered separately from the rest of more 'regular' megathrust earthquakes.

This behaviour raises another important question regarding tsunami potential of subduction zones where no large historical event has been documented (e.g, a segment of subduction zone south of Sanriku in Japan). Because most seismic and tsunami hazard mitigation measures heavily rely on the past experience, such 'quiet' subduction zones tend to receive less attention, but slow accumulation of strain in such subduction zones can lead to extremely serious, though infrequent, tsunami hazard, and special attention needs to be paid to such possibilities.

8 CONCLUSION

We have shown that even if old seismograms are few with poorly documented characteristics, we can use them to clarify certain aspects of important historical earthquakes.

From the waveforms and the amplitude of Omori and Wiechert seismograms, we could determine that the 1907 Sumatra earthquake was probably a thrust earthquake on the plate boundary, not an outer-rise earthquake as inferred from the location given by Gutenberg & Richter (1954). The magnitude is still uncertain but up to a period of 40 s, it is probably 7.8 (meaning between 7.5 and 8) with some indication of increasing size with period from 10 to 40 s. We note, however, because of the limited number and quality of old seismograms, our conclusion is subject to considerable uncertainty and should be taken with caution. We tried to present as much raw

data as possible to allow other investigators to examine them if some aspects of the conclusions are questioned.

If more seismograms with well-documented instrument characteristics are available, we would be able to harden our conclusion. The current situation (Lee & Benson 2008), however, is alarming because old seismograms are being discarded at many seismological observatories and institutions because of the space, budgetary and personnel limitations. We hope that this study has demonstrated the value of old seismograms for unravelling key characteristics and diversity of subduction-zone earthquakes which can be understood well only from data over an extended period of time. A better understanding of the diversity of subduction-zone earthquakes is critically important for implementing comprehensive hazard mitigation measures.

ACKNOWLEDGMENT

We thank our colleagues at many seismological institutions and observatories who helped us explore the availability and collect valuable historical seismograms. Just to mention a few: Conny Holmqvist, Kazuko Noguchi, Kenshiro Tsumura, Nobuo Hamada, Norihito Umino, Satoshi Hirahara, Torsten Dahm, Martin Leven, Thomas Jahr, Dieter Kurrle, Zhu Yuanqing, Thierry Camelbeeck, Suhardjono, Randell Teodoro, Antoniuo Pazos, Bernard Dost, Brian Ferris, and Zurab Javakhishvili. Michel Cara helped us understand the polarity convention of Wiechert seismographs. We have benefited a great deal from discussions with William McCann who also provided us with the base map for Fig. 2. We thank Kerry Sieh, William McCann and Johannes Schweitzer for providing us with helpful comments during the final revision process. We thank Doug Dodge for coding the JLoc grid-search earthquake location program. The copies of the pages of the Gutenberg notepad used in this study were provided by the Archives of the California Institute of Technology. We thank the IRIS Data Management Center for providing us access to the global broad-band sesimograms. We thank the National Research Institute for Earth Science and Disaster Prevention (NIED) Japan for providing us access to the F-net broad-band seismograms. Archiving and scanning project of Mizusawa seismograms was supported by Grant (PR2002) 'The Research on the Tonankai and Nankaido earthquakes' from the ministry of Education, Culture, Science and Technology of Japan.

REFERENCES

Abe, K., 1981. Magnitudes of large shallow earthquakes from 1904 to 1980, *Phys. Earth planet. Inter.,* **27,** 72–92.

Ammon, C.J., Kanamori, H. & Lay, T., 2008. A great earthquake doublet and seismic stress transfer cycle in the central Kuril islands, *Nature,* **451,** 561–565.

Ando, M., 1975. Source mechanisms and tectonic significance of historical earthquakes along the Nankai trough, Japan, *Tectonophysics,* **27,** 119–140.

Briggs, R.W. *et al*., 2006. Deformation and slip along the Sunda Megathrust in the great 2005 Nias-Simeulue earthquake, *Science,* **311,** 1897–1901.

Bungum, H., Pettenati, F., Schweitzer, J., Sirovich, L. & Faleide, J.I., 2009. The 23 October 1904 M_S 5.4 Oslofjord earthquake: Reanalysis based on macroseismic and instrumental data, *Bull. seism. Soc. Am.,* **99,** 2836–2854.

Charlier, C. & Van Gils, J.M., 1953. *Liste des Stations Seismologiques Mondiales,* Available at: http://www.iris.edu/seismo/info/stations/Charlier1953.pdf] in 2 volumes, no page number, Observatoire Royal de Belgique, Uccle.

Crotwell, H.P., Owens, T.J. & Ritsema, J., 1999. The TauP Toolkit: flexible traveltime and ray path utilities, *Seism. Res. Lett.,* **70**(2), 154–160.

Geiger, L.C., 1912. Probability method for the determination of earthquake epicenters from the arrival time only, *Bull. St. Louis Univ.,* **8,** 60–71.

Geller, R.J. & Kanamori, H., 1977. Magnitudes of great shallow earthquakes from 1904 to 1952, *Bull. seism. Soc. Am.,* **67,** 587–598.

Goodstein, J.R., Kanamori, H. & Lee, W.H.K., 1980. Seismology microfiche publications from the Caltech archives, *Bull. seism. Soc. Am.,* **70,** 657–658.

Gutenberg, B., 1945. Amplitudes of surface waves and magnitudes of shallow earthquakes, *Bull. seism. Soc. Am.,* **35,** 3–12.

Gutenberg, B. & Richter, C.F., 1954. *Seismicity of the Earth and Associated Phenomena,* 2nd edn, p. 310, Princeton Univ. Press, Princeton.

Gutenberg, B. & Richter, C.F., 1956. Magnitude and energy of earthquakes, *Ann. Geofis., (Rome),* **9,** 1–15.

Hsu, Y.-J. *et al*., 2006. Frictional afterslip following the 2005 Nias-Simeulue earthquake, Sumatra, *Science,* **312,** 1921–1926.

Imamura, A., 1928. On the seismic activity of central Japan, *Jpn. J. astr. Geophys.,* **6,** 119–137.

Ishibashi, K., 1981. Specification of a soon-to-occur seismic faulting in the Tokai District, central Japan, based on seismotectonics. in *Earthquake Prediction: An International Review Maurice Ewing Ser.,* Vol. 4, pp. 297–332, eds Simpson, D.W. & Richards, P.G., American Geophysical Union, Washington, DC.

Jeffreys, H. & Bullen, K.E., 1940. *Seismological Tables*. British Association for the Advancement of Science, London.

Kanamori, H., 1971. Seismological evidence for a lithospheric normal faulting–the Sanriku earthquake of 1933, *Phys. Earth planet. Inter.,* **4,** 289–300.

Kanamori, H., 1972. Mechanism of Tsunami earthquakes, *Phys. Earth planet. Inter.,* **6,** 346–359.

Kennett, B.L.N. & Engdahl, E.R., 1991. Traveltimes for global earthquake location and phase identification, *Geophys. J. Int.,* **105,** 429–465.

Kennett, B.L.N., Engdahl, E.R. & Buland, R., 1995. Constraints on seismic velocities in the Earth from traveltimes, *Geophys. J. Int.,* **122,** 108–124.

Konca, A.O. *et al*., 2008. Partial rupture of a locked patch of the Sumatra megathrust during the 2007 earthquake sequence, *Nature,* **456,** 631–635, doi:610.1038/nature07572.

Konca, A.O. *et al*., 2007. Rupture kinematics of the 2005 Mw 8.6 Nias-Simeulue earthquake from the joint inversion of seismic and geodetic data, *Bull. seism. Soc. Am.,* **97,** S307–S322.

Kozák, J., 2001. 100-year anniversary of the first international seismological conference, *Studia geoph. et geod.,* **45,** 200–209.

Lay, T. *et al*., 2005. The great Sumatra-Andaman earthquake of 26 December 2004, *Science,* **308,** 1127–1133.

Lee, W.H.K. & Baker, L.M., 2006. Development of a direct search software package for locating poorly constrained earthquakes (abstract), *Seism. Res. Lett.,* **77,** 291–292.

Lee, W.H.K. & Benson, B.R., 2008. Making non-digital-recorded seismograms accessible online for studying earthquakes, in *Historical Seismology,* pp. 403–427, eds J. Frechet, J., Meghraoui, M. & Stucchi, M., Springer, Berlin.

Lee, W.H.K. & Dodge, D.A., 2007. Development of a direct search software package for poorly constrained earthquakes, in *Seismology Technical Report,* pp. 6–27, Central Weather Bureau, Taiwan.

Matuzawa, T., 1942. Seismometrische Untersuchungen des Erdbebens vom 2. Marz 1933. : IV. Raumverteilung der Wellenstrahlung aus dem Herd, in *Bulletin of Earthquake Research Institute,* Vol. 20, pp. 162–171, Tokyo University.

McAdoo, B.G., Dengler, L., Prasetya, G. & Titov, V., 2006. How an oral history saved thousands on Indonesia's Simeulue Island during the December 2004 and March 2005 tsunamis, *Earthq. Spectra,* **22,** S661–S669.

Monecke, K., Finger, W., Klarer, D., Kongko, W., McAdoo, B.G. & Moore, A.L., 2008. A 1,000-year sediment record of tsunami recurrence in northern Sumatra, *Nature,* **455,** 1232–1234.

Natawidjaja, D.H., Sieh, K., Ward, S.N., Cheng, H., Edwards, R.L., Galetzka, J. & Suwargadi, B.W., 2004. Paleogeodetic records of seismic

and aseismic subduction from central Sumatran microatolls, Indonesia, *J. geophys. Res.,* **109,** B04306, doi:10.1029/2003JB002398.
Newcomb, K.R. & McCann, W.R., 1987. Seismic history and seismotectonics of the Sunda arc, *J. geophys. Res.,* **92,** 421–439.
Press, W.H., Flannery, V, Teukolsky, S.A. & Vetterling, W.T., 1986. *Numerical Recipes: The Art of Scientific Computing,* Cambridge Univ. Press, Cambridge.
Omori, F., 1907. Notes on the Valparaiso and Aleutian earthquakes of August 17, 1906, *Bulletin of the Imperial Earthquake Investigating Committee,* vol. 1, pp. 75–113.
Osaka Observatory, 1908. Report on Omori Horizontal Pendulum Seismograph Observations in Osaka for the Two Years 1906–1907.
Richter, C.F., 1958. *Elementary Seismology,* pp. 768, W. H. Freeman, San Francisco.
Royal Magnetic and Meteorological Observatory, Batavia, 1909. Vulkanische verschijnselen en aardbevingen in den Oost-Indischen Archipel waargenomen gedurende het jaar 1907, in *Natuurkundig Tijdschrift voor Nederlandsch-Indie,* pp. 117–201, ed. Bemmelen, W.V., Nederlandsch-Indie utigeven door de Koninklijke Natuurkundige Vereeniging in Nederl-Indie, Welevreden.
Sieh, K. *et al*., 2008. Earthquake supercycles inferred from sea-level changes recorded in the corals of west Sumatra, *Science,* **322,** 1674–1678.
Sladen, A., Avouac, J.-P., Meltzner, A.J., Genrich, J.F., Galetzka, J.E., Sieh, K.E. & Natawidjaja, D.H., 2009. Source model of the 2008, Mw = 7.4, Simeulue, Indonesia earthquake (abstract), *T23B-1926, AGU Fall Meeting,* 2009.
Szirtes, S., 1912. Registrierungen der besser ausgeprägten seismischen Störungen des Jahres 1907, Ergänzung zum seismischen Katalog. Veröffentlichungen des Zentralbureaus der Internationalen Seismologischen Assoziation. Serie B, Kataloge, Strassburg, pp. 1, 5–7.
Tilmann, F.J., Craig, T.J., Grevemeyer, I., Suwargadi, B., Kopp, H. & Flueh, E., 2010. The updip seismic/aseismic transition of the Sumatra megathrust illuminated by aftershocks of the 2004 Aceh-Andaman and 2005 Nias events, *Geophys. J. Int.,* **181,** 1261–1274, doi:1210.1111/j.1365-1246X.2010.04597.x.
Visser, S.W., 1922. Inland and Submarine Epicentra of Sumatra and Java earthquakes, *Koninklijk Magnetisch en Meteorologisch Observatorium te Batavia,* **9,** 1–14.

APPENDIX A: NOTE ON THE EPICENTRAL LOCATION

Szirtes (1912) provides the most complete list of arrival times for the 1907 earthquake, and an epicentre location at 2.00°N and 96.25°E based on a report by T. H. Staverman. This epicentre differs significantly from the epicentre location published by Gutenberg & Richter (1954) at 2.00°N and 94.50°E. Just to get some ideas about the uncertainty in location, we used the JLoc interactive, direct-search, location software (Lee & Baker 2006; Lee & Dodge 2007), and relocated the hypocentre. The JLoc program allows the user to choose several different velocity models (including the Jeffreys & Bullen's (1940) and several modern ones, such as iasp91 by Kennett & Engdahl 1991, and ak135 by Kennett *et al.* 1995), and is capable of computing station residuals (using the TauP traveltime calculator by Crotwell *et al.* 1999), and their rms values from a specified hypocentre, thereby performing a grid-search on a user specified 3-D space grid for a "best fit" solution. JLoc also includes a simplex algorithm (Press *et al.* 1986) to 'home' in for a final solution.

Because of large uncertainty in the station clock before radio time signals became available in the 1920s, locating an earthquake using P- and/or S-arrival times using the standard Geiger (1912) method is difficult. The use of S-P and SKS-P traveltimes avoids the station clock problem, but the location accuracy still depends on how accurately the P and S (or SKS) phases were 'picked', which in turn depends on the clarity of the seismic phases and the time mark resolution of the seismograms. For a S-P (and SKS-P) relocation, we selected 12 well-distributed stations from a total of 42 available stations. We added arrival times of Uppsala, Honolulu, and Sitka from their station bulletins to the compilation of Szirtes (1912). These selected data are shown in Table A1. For comparison, the rms values computed for the Gutenberg & Richter's (1954) location and the Staverman's location are shown in Table A2.

Table A1. Observed traveltime for S-P or SKS-P from 12 well-distributed selected stations.[a]

Station name	Delta (degree)	Azimuth (degree)	Phase	Observed Traveltime (s)	Code
Simla	34.09	330.0	S-P	336.	SMI
Zi-ka-wei	37.52	36.8	S-P	351.	ZKW
Perth	38.53	152.8	S-P	378.	PER
Osaka	48.89	43.8	S-P	421.	OSA
Irkutsk	50.51	6.4	S-P	450.	IRK
Tiflis	60.67	317.9	S-P	504.	TIF
Pulkova	76.25	331.7	S-P	580.	PUL
Capetown	80.97	235.3	S-P	612.	CTO
Messina	81.40	308.2	S-P	607.	MES
Uppsala	82.46	330.1	S-P	613.	UPP
Göttingen	86.04	321.4	S-P	628.	GTT
Honolulu	103.82	67.5	SKS-P	624.	HON

Note: [a]Delta is the epicentral distance (in degrees) from 2° 00' N and 96° 15'E, and Azimuth is from the epicentre to the station measured from the North in degrees.

Table A2. Comparison of epicentre locations by different authors (rms value is computed using the residuals of the same set of stations given in Table A1, and a modern velocity model, AK135 by Kennett *et al.* 1995). A focal depth of 20 km is assumed for all solutions.

Author (reference)	Latitude	Longitude	rms (sec)
Staverman (Szirtes 1912)	2.00N	96.25E	8.15
Gutenberg & Richter (1954)	2.00N	94.50E	9.41
This study	2.48N	96.11E	7.80

We conclude that the available arrival time data in1907 are so poor (probable picking error of about 10 s for Milne seismograms or about 3 s for Omori or Wiechert seismograms; in addition, there were large clock errors, exceeding tens of seconds at some stations) that epicentre location has an error of at least 1°. The epicentre thus relocated is at (2.48°N, 96.11°E). The 95 per cent confidence ellipse parameters are: Semi-major axis length = 290 km; Semi-minor axis length = 223 km, and strike of semi-major axis = 69°.

APPENDIX B: MAGNITUDE ESTIMATION

The 2002 Sumatra and 2008 Sumatra earthquakes are given M_S = 7.6 and 7.5, respectively, in the USGS report. Since, the current practice of M_S determination is slightly different from the practice used by Gutenberg & Richter (1954), and since the number and azimuthal coverage of stations used in these determinations are unknown, we estimated M_S using all the broad-band stations as follows. We bandpass filter the vertical component of displacement over a narrow frequency band between 0.04 to 0.06 Hz, and measure the peak amplitude, A_z. Then, we use the IASPEI formula

$$M_S = \log(A_z/T) + 1.66\log\Delta + 3.3$$

with $T = 20$ s. This formula is supposed to be used for the amplitude measured from the horizontal component, but Abe (1981) found

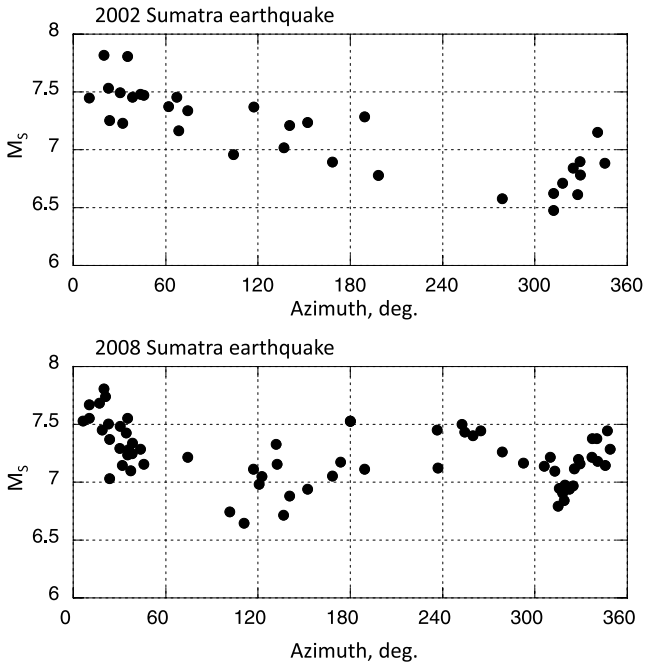

Figure B1. Azimuthal distribution of M_S of the 2002 and 2008 Sumatra earthquakes determined from bandpassed records.

no systematic difference in M_S whether the horizontal or vertical components are used. Then, to conform to the original definition of Gutenberg (1945), we subtract 0.18 following the suggestions by Geller & Kanamori (1977) and Abe (1981).

The results are shown in Fig. B1. For the 2008 event for which many stations are available, the effect of radiation pattern is evident. A similar, but incomplete, trend is seen for the 2002 event. The average M_S is 7.15 and 7.23 for the 2002 and 2008 events, respectively. We use these values as reference.

APPENDIX C: AVAILABILITY OF SEISMOGRAMS

We have contacted the observatories and institutions at the following locations (some are old names): Japan Meteorological Agency, Mizusawa Observatory, Earthquake Research Institute (Tokyo University), Hamburg, Göttingen, Jena, Stuttgart, Strasbourg, Uppsala, Zikawei, Uccle, Batavia, Manila, San Fernando, Ebro, De Bilt, Christchurch, and Tbilisi. For the 1907 earthquakes, we could obtain records only from Osaka Observatory (hand-drafted copy), Mizusawa (Omori), Earthquake Research Institute (Omori), Göttingen (Wiechert), Potsdam 9probably Wiechert), Hamburg (Wiechert), Uppsala(Wiechert), Strasbourg (microfilm Wiechert), and San Fernando (Milne). The stations and institutions we contacted in this study are listed in Table C1.

Figure C1. (a) Professos Fusakichi Omori and Emil Wiechert at the occasion of the Internationale Seismologische Conferenz held in Strassburg, April 11–13, 1901 (Kozák (2001), with permission). (b) Omori seismograph (horizontal) and Wiechert seismograph (horizontal).

Considering the historical importance of the old seismograms, we include a photograph of Professors Wiechert and Omori sitting side by side at a rare occasion, and the seismographs to which their names are attached in Fig. C1.

Table C1. List of stations and institutions contacted in this study. Contact information and the status of archive are also included.

Station	1907 Sumatra record	Institution	Name – e-mail – URL	Note
Osaka, Japan	Omori (copy)			
Mizusawa, Japan	Omori (EW, NS)	Mizusawa Latitude Observatory		In good condition
Tokyo (Hongo), Japan		Earthquake Research Institute	Dr. Kenji Satake satake@eri.utokyo.ac.jp www.eri.u-tokyo.ac.jp	Many Omori seismograms in good condition
Hamburg, Germany	Wiechert (H)	Institut für Geophysik, Universität Hamburg	Dr. Torsten Dahm http://www.geophysics.zmaw.de	Very complete collection Wiechert: 1905–1942, 1952–1974 Hecker: 1906–1928
Göttingen, Germany	Wiechert (H)	Institut für Geophysik, Universität Göttingen	www.geo.physik.uni-goettingen.de	Very complete collection Wiechert: 01-1903 to 06-2005
Stuttgart, Germany	No record	Institut für Geophysik, Universität Stuttgart	Dr. Rudolf Widmer-Schnidrig widmer@geophys.uni-stuttgart.de	Fairly complete collection Omori-Bosch since 1905 Wiechert since 1937
Jena, Germany	No record	Institut für Geowissenschaften, Universität Jena	www.geo.uni-jena.de	Records from the Jena and Potsdam observatories; see www.geo.uni-jena.de/geophysik/home/archiv.html
Strasbourg, France	Wiechert (H)	Ecole et Observatoire de Sciences de la Terre	Dr. Luis Rivera luis.rivera@unistra.fr eost.u-strasbg.fr	Microfilm (often poor): Wiechert (1904–1930), Galitzin (1914–1915, 1922–1930), 19Ton (1926–1930) Selected original records: Wiechert (1930–1968), Galitzin (1930–1975), 19Ton (1930–1968), Mainka (1921–1924)
Uppsala, Sweden	Wiechert (H)	Department of Earth Sciences, Uppsala University	www.geofys.uu.se	Very complete Wiechert collection
Zikawei, China	No record	Shanghai Seismological Bureau		
Uccle, Belgium	No record	Observatoire Royal de Belgique	Dr. Thierry Camelbeeck T.Camelbeeck@oma.be seismologie.oma.be	Fairly complete Wiechert: 1910–1949, Galitzin (H): 1911–1950 Willip-Somville (Z): 1930–1950

Table C1. *(Continued).*

Station	1907 Sumatra record	Institution	Name – e-mail – URL	Note
Batavia, Indonesia	No record	Meteorological and Geophysical Agency	www.bmg.go.id	
Manila, Philippines	No record	Manila Observatory	Dr. Fr. Segio S. Su, SJ su@observatory.ph www.observatory.ph	All the seismological records were destroyed during World War II
San Fernando, Spain	Milne published copy	Real Instituto y Observatorio de la Armada	www.roa.es	
Ebro, Spain	No record	Observatorio de l'Ebre	www.obsebre.es	Very complete collection Vicentini: 1905–1936, Grablovitz: 1905–1918, Mainka: 1916–1970
De Biltt, the Netherlands	No record	The Royal Netherlands Meteorological Institute	Dr. Bernard Dost Bernard.Dost@knmi.nl www.knmi.nl	Very complete collection of Galitzin records since 1912 (2 hor., +Z since 1922) Fairly complete collection (1908–1913 and 1939–1958) of Wiechert (200 kg), and less complete (1908–1957) collection for the Bosch instrument
Christchurch, New Zealand	No record	Institute of Geological and Nuclear Sciences	Dr. Brian Ferris B.Ferris@gns.cri.nz www.gns.cri.nz	Nearly complete collection of Christchurch Milne records for 1902 to 1932, and Galitzin ZNE from 1930 to 1957
Tbilisi, Georgia	No record	Seismic Monitoring Centre of Georgia	seismo.iliauni.edu.ge	
Samoa, Samoa	Hardly readable	Institut für Geophysik, Universität Göttingen	www.geo.physik.uni-goettingen.de	Preserved in Göttingen Wiechert: 16.12.1902 to 1.6.1913